Biochemical and Biophysical Research Communications 425 (2012) 201–206

Contents lists available at SciVerse ScienceDirect

Biochemical and Biophysical Research Communications

journal homepage: www.elsevier.com/locate/ybbrc

Biophysical studies with AICD-47 reveal unique binding behavior characteristic of an unfolded domain

Samir Das [a], Saptaparni Ghosh [b], Dipak Dasgupta [b], Udayaditya Sen [c,*], Debashis Mukhopadhyay [a,*]

[a] Structural Genomics Division, Saha Institute of Nuclear Physics, 1/AF Bidhan Nagar, Kolkata 700 064, WB, India
[b] Biophysics Division, Saha Institute of Nuclear Physics, 1/AF Bidhan Nagar, Kolkata 700 064, WB, India
[c] Crystallography and Molecular Biology Division, Saha Institute of Nuclear Physics, 1/AF Bidhan Nagar, Kolkata 700 064, WB, India

ARTICLE INFO

Article history:
Received 4 July 2012
Available online 22 July 2012

Keywords:
Alzheimer's disease
Intrinsically unstructured protein
Conformational switch
AICD-47
Fluorinated alcohol

ABSTRACT

APP intracellular C-terminal domain (AICD-47), generated upon γ-secretase cleavage of Amyloid precursor's protein (APP), bears the signature of a classical intrinsically unstructured domain (IUD). Comparing the recent crystal structures of AICD-47 peptides bound to its different adaptors such as protein-tyrosine-binding domain-2 (PTB2) of Fe65 and Src homology 2 (SH2) domain of growth factor receptor binding protein 2 (Grb2), the "conformational switching" of AICD-47 becomes evident. In order to understand different binding processes undertaken by this flexible molecule, upon recognizing different interfaces resulting in different 3D conformations, spectroscopic and calorimetric studies have been done. CD spectroscopy has revealed an overall random coil like structure in different pHs while TFE (2′-2′-2′-trifluoro ethanol) and HFIP (Hexa fluoro isopropanol) induced α-helicity to a certain extent. Binding of Tyr phosphorylated AICD-47 (^{P}AICD-47) to Grb2-SH2 domain was carried out by a favorable enthalpic change ($\Delta H = -197.5 \pm 6.2$ kcal mole^{-1} at 25 °C) and an unfavorable entropic contribution ($\Delta S = -631$ cal mol^{-1} deg^{-1} at 25 °C). Alternative conformation of AICD-47 in different biological contexts is another remarkable feature of IUDs which presumably has definitive roles in regulating Alzheimer's disease phenotype.

1. Introduction

Though the classical paradigm of "sequence–structure–function" is valid for most of the proteins, "intrinsically unstructured domains" (IUDs) are exceptions, being devoid of any compact globular folds and being capable of innumerable functional possibilities [1]. IUDs possess a large net charge at neutral pH with low abundance of hydrophobic amino acids [2]. The structural randomness or 'entropy' decreases dramatically upon binding to specific partners where coupled folding and binding allows burial of an exposed surface area even with small interacting domains and generate complexes with high specificity and relatively low affinity, a feature of these proteins [3–5].

Amyloid precursor's protein (APP), a type-I transmembrane protein, with a large extracellular amino-terminal domain and a shorter carboxy-terminal cytosolic tail, is involved in Alzheimer's disease (AD) pathogenesis. Comparing the crystal structures of the Carboxy terminal tail (AICD-47 or APP 649–695, as of APP-695 isoform numbering) peptides bound to its different adaptors like Fe65-PTB2 and Grb2-SH2 domains, a "conformational switching" of AICD-47 is reckoned [6,7]. Both in acidic and alkaline pH, AICD-47 does not possess any tertiary contacts, typical of an IUD, and shows somewhat folded stable conformation with only hydrophobic side chain clusters. The domain is significantly enriched in Glu, Lys, His and other charged amino acids and depleted of hydrophobic or order promoting residues like Trp and Cys. Moreover, the AICD-47 fragment possesses several short eukaryotic linear motifs (ELM), responsible for associating with different binding partners. These transitory conformers are stabilized and rearranged upon binding [8]. The available NMR conformations do point out the inherent flexibility of the molecule, although prove to be inadequate in terms of explaining the molten-globule formation and the underlying thermodynamics [8]. The crystal structures of Grb2-SH2 domain bound peptides have revealed the consensus recognition motif as 'pY-X-N-X' (where 'X' is any amino acid) where the protein–peptide interactions are stabilized by a network of hydrogen bonds mediated by conserved Arg, Ser, Thr with PTR and backbone atoms of peptide. With the exception of AICD-47, where Pro is present at pY + 3 position, all other peptides bound to Grb2-SH2 domain possess Val at the equivalent position [6].

Abbreviations: APP, amyloid precursor's protein; AICD, APP-intracellular C-terminal domain; AD, Alzheimer's disease; SH2, Src homology 2; PTR and pY, phosphorylated tyrosine; IUD, intrinsically unstructured domain; Grb2, growth factor receptor binding protein 2, TFE, 2′-2′-2′-trifluoro ethanol; HFIP, hexa fluoro isopropanol.

* Corresponding authors. Fax: +91 33 2337 4637.
E-mail addresses: udayaditya.sen@saha.ac.in (U. Sen), debashis.mukhopadhyay@saha.ac.in (D. Mukhopadhyay).

0006-291X/$ - see front matter © 2012 Elsevier Inc. All rights reserved.
http://dx.doi.org/10.1016/j.bbrc.2012.07.067

Thermodynamic investigation of the interaction of Shc-derived phosphotyrosine hexapeptide 'Ac-S^{P}YVNVQ-NH2' with Grb2-SH2 reveals both an enthalpically and entropically favorable event, the enthalpic contribution coming primarily from the PTR and Asn (pY + 2) residues and significant entropic contributions arising from the Val (pY + 1) residue [9]. Understanding the binding thermodynamics of AICD-47, therefore, becomes interesting in presence of a hydrophobic Pro, instead of usual Val, located at the core of the binding interface.

Water miscible alcohols like TFE (2′-2′-2′-trifluoro ethanol) and HFIP (hexa fluoro isopropanol) are known to form micelle-like assemblies where hydrophobic groups, buried deep inside, cause diminution of polarity around the polypeptide chain; eventually stabilizing local hydrogen bonds and generating amphiphilic α-helix [10]. The dielectric constant of water-alcohol mixture is closer to protein interior, which could alleviate the interaction of charged groups and might be adequate to build up pre-α-helical conformations having high propensity for helix formation [11,12]. On the other hand, several reports suggest that peptide fragments and proteins differing vastly in their amino acid composition, can be converted into amyloid-like β fibrils and β-sheets in presence of varying amounts of TFE and HFIP [13–20].

The aim of the present study is to understand the thermodynamic basis of binding of unstructured AICD-47 fragment. Addition of TFE or HFIP causes considerable changes into the secondary structural elements of AICD-47, transforming its native random coil like unstructured conformation to α-helical entity. Entropic and enthalpic contributions of Tyr phosphorylated AICD-47 (^{P}AICD-47) upon binding to Grb2-SH2 domain has also been measured to evaluate which thermodynamic parameter drives the complex formation. Understandably, rapid switching of cognate partners in cellular pathways, as evidenced in AICD-47, could contribute to the disease pathogenesis.

2. Materials and methods

2.1. Purification of proteins

Cloning, expression and purification of Grb2-SH2 domain along AICD-47 were described in details before [6]. To obtain Tyr-phosphorylated AICD-47 (^{P}AICD-47), the construct was transformed into pTK-BL21 (DE3) (also known as TKB1, obtained from Stratagene,) strain of *Escherichia coli* acquiring a plasmid which encodes tyrosine kinase Elk (EphB1) gene. The transformation of AICD-47 in TKB1 was performed following the manufactures guideline and grown in LB broth containing appropriate antibiotics at 37 °C. Cells were collected by centrifugation and resuspended in induction medium, containing 1 mM IPTG and 10 mg/ml β-indole acrylic acid, to induce expression of the ephB1 gene. Cells were grown for an additional 3 h at 37 °C, harvested by centrifugation and sonicated in presence of 50 mM Tris–Cl (pH 8.0), 200 mM NaCl, 100 mM sodium orthovanadate and 50 mM sodium fluoride [21]. Like non-phosphorylated AICD-47, the phosphorylated ^{P}AICD-47 was concentrated up to 1 mg/ml in similar buffer and Tyr phosphorylation was confirmed by 4G10 Anti-Phosphotyrosine antibody (Millipore, India).

2.2. Circular dichroism measurement

CD spectra were recorded on a CD spectrometer of BioLogic Science Instruments (France) using a rectangular quartz cell of pathlength of 0.1 mm at 293 K. Measurements were taken at wavelengths between 190 and 280 nm at a scan rate of 3 nm/min. A total of three scans were averaged to obtain each spectrum and they were baseline subtracted for buffer. 10 μM of AICD-47 was taken for each measurement at pH 4.0 (50 mM potassium acetate), pH 6.0 (50 mM Mes) and pH 8.0 (50 mM Tris) with 300 mM NaCl. TFE and HFIP, obtained from Fluka (Sigma Aldrich), were also used as solvents to check their influence on AICD-47 structure. The percentage of helicity was estimated by standard protocol using K2D3 server [22].

2.3. Isothermal titration calorimetry

Isothermal titration calorimetry (ITC) measurements were performed with an ITC-200 (Microcal, Northampton, MA, USA) in 20 mM Mes plus 300 mM NaCl, pH 6.5 at two different temperatures: 20 and 25 °C. Titration curves were fit by using the ORIGIN program supplied by the manufacturer. For all experiments, the heat of the dilution for the individual reactions was determined by titration of into the buffer and buffer into Grb2-SH2 domain. The heat of dilution of buffer into Grb2-SH2 domain was appropriately subtracted. The stoichiometry, binding constant (K_B) and enthalpy changes were determined from a fit of the observed heat change as a function of the concentration of ^{P}AICD-47. The corresponding free energy change (ΔG) and entropy change (ΔS) upon ligand binding were calculated from the following relation:

$$-RTlnK_B = \Delta G = \Delta H - T\Delta S \quad (1)$$

R is the gas constant, and T is the absolute temperature. These parameters permit better thermodynamic characterization of the nature of the binding reaction.

As cratic water molecules could also contribute to the binding of unfolded protein molecule, the apparent binding constant (K_B^{app}) was also determined to make out their involvement in overall binding process [23].

$$K_B = (K_B^{app} \times C_w), \text{ where } C_w \text{ is the concentration of water, } 55.5 \text{ mol/L at } 25^{\circ}\text{C}. \quad (2)$$

3. Results

3.1. Circular dichroism of AICD-47 in different conditions

AICD-47, in the absence of any solute, showed considerable unfolded secondary structure in aqueous solution as measured by CD spectroscopy (Fig. 1A). On an average, around 75% of the protein remained as random coil in three different pH values (Table 1). A shift in the spectral minimum was noticed: 200 nm at pH 4.0, 208 nm at pH 6.0 and 197 nm at pH 8.0, respectively, with a linear increase in the spectral intensity in the same order and without any concomitant change in the secondary structure content (Table 1). Addition of TFE caused significant changes in the CD spectra, consistent with reduction of random coil conformation and formation of secondary structures with large contributions from α-helical motif (Fig. 1B). Upon addition of 40% (v/v) TFE, the spectrum became indicative of a helical conformation, with the minimum shifting to 209 nm ($\pi\pi*$ transition) and considerable negative ellipticity being developed at 222 nm ($n\pi*$ transition). Thus for AICD-47, TFE acted as a helix inducing solvent, as expected, and the presence of an isodichroic point (200 nm) where intersections of four spectra were initiated, indicated a simple random coil/helix transition [24].

As an example of the effect of HFIP on an unfolded polypeptide, the HFIP-dependent conformational transition of AICD-47 was also studied (Fig. 1C). The far-UV CD spectra in presence of various concentrations of HFIP showed, similar to that of TFE, that HFIP stabilized the helical conformation and decreased the amount of random coil in AICD-47 as well (Table 1). However, in presence of 20% (v/v) HFIP, AICD-47 showed ~22% β-sheet formation, higher from its conformation at pH 8.0 without any solvent. The addition

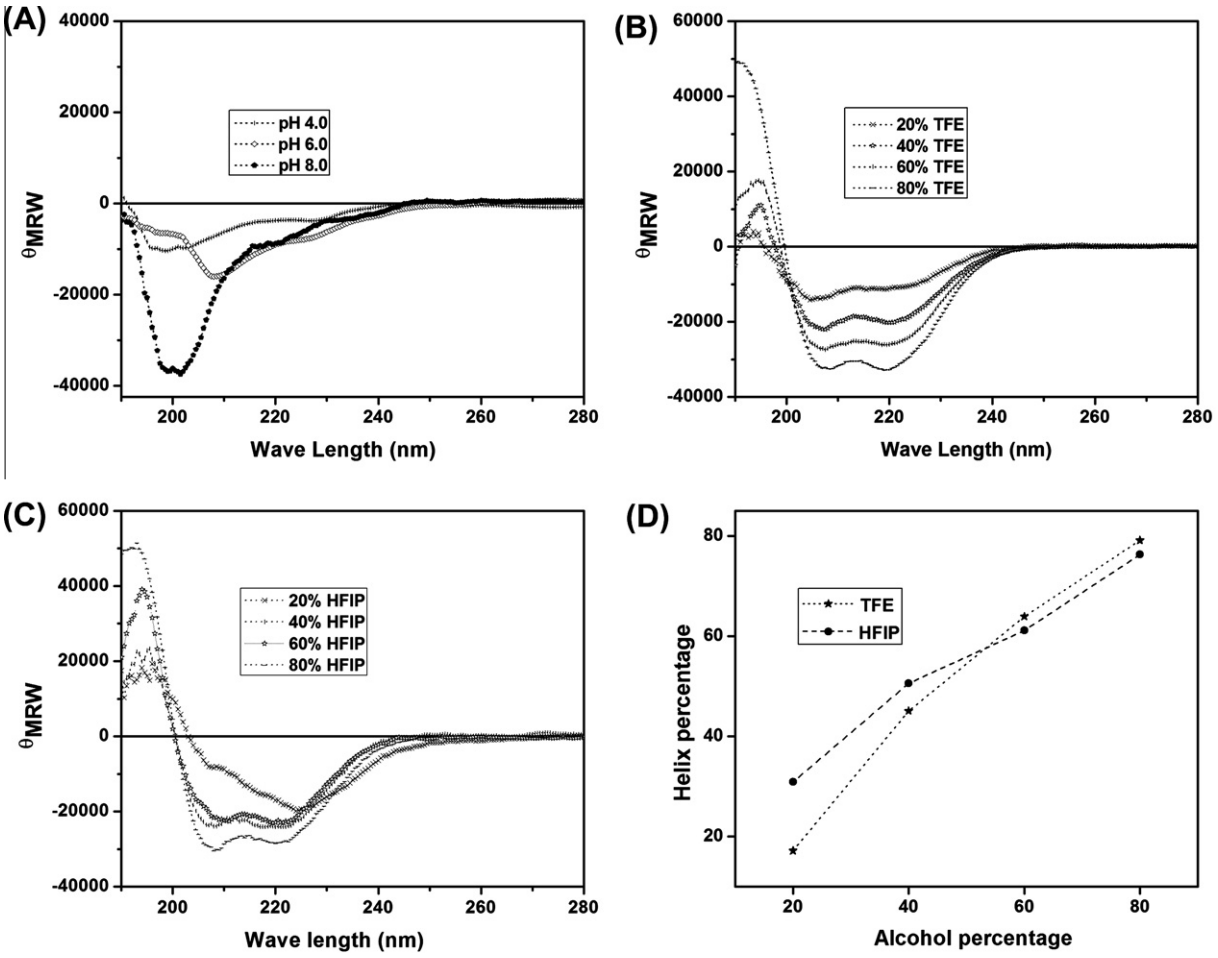

Fig. 1. Low-ultraviolet CD spectra of AICD-47. Data were acquired at different pH (A) and various concentrations of TFE (B) and HFIP (C) solution at 20 °C, respectively. The molar ellipticity is in deg cm^2 $dmol^{-1}$. The percentage of helicity as obtained from K2D3 server with respect to TFE and HFIP concentrations are also provided in (D).

Table 1
Quantitative analysis of the secondary structure content in AICD-47 under different pH and different concentrations of solvents using K2D3 server.

Condition	% of α-Helicity	% of β-strand	% of coil
pH 4.0	6	15	79
pH 6.0	7	18	75
pH 8.0	3	21	76
20% TFE	17	14	67
40% TFE	45	5	50
60% TFE	64	0	36
80% TFE	79	0	21
20% HFIP	31	22	47
40% HFIP	51	5	44
60% HFIP	61	5	34
80% HFIP	76	0	23

of HFIP at more than 20% (v/v) converted the spectrum radically towards α-helical conformation with minima at 208 and 222 nm. Apart from 20%, all other concentrations of HFIP showed the presence of an isodichroic point at 200 nm, similar to TFE, indicating almost similar coil to helix transition. The maximum ellipticities observed for these two alcohols were almost similar, indicating that the maximum helical content, estimated to be 80%, is independent of the alcohol species. The helicity increment of AICD-47 with increasing the concentration of fluorinated alcohol is almost indistinguishable as shown in Fig. 1D. This indicates that the denaturation potential of an alcohol is closely correlated with its potential for stabilizing the helical conformation in the unfolded protein, suggesting that the mechanisms responsible for the two processes are identical.

3.2. Isothermal titration calorimetry of ^{P}AICD-47 with Grb2-SH2 domain

Thermodynamic parameters such as the Gibbs free energy change (ΔG), enthalpy change (ΔH), and entropy change (ΔS) along with the number of binding sites (N) and binding constant (K_B) can provide useful information for identifying fundamental forces involved in protein–protein interaction where "conformational switching" of an unstructured protein is commenced upon binding. Furthermore, in contrast to other Grb2-SH2 bound peptides, ^{P}AICD-47 possessed Glu and Pro residues at pY + 1 and pY + 3 positions, respectively, making the process unique.

A typical binding isotherm of the ^{P}AICD-47 showed that the binding of the unstructured protein at 20 °C to be highly exothermic (ΔH = −384.5 ± 15.4 kcal $mole^{-1}$) (Fig. 2A). Curve fitting of such binding isotherms depicted that the stoichiometry of the phosphoprotein binding to the Grb2-SH2 domain was 1:1. The binding constant (K_B) at 20 °C was 8.23 ± 1.73 × 10^5 M^{-1}, corresponding to a dissociation constant (K_D) of 1.2 μM. At 20 °C the free energy of binding (ΔG) and entropic change (ΔS) were −7.92 and −1.28 kcal $mol^{-1}deg^{-1}$, respectively. The apparent binding constant (K_B^{app}) which was solely contributed by protein–protein interactions and devoid of the influence of associated water molecules was 1.5 × 10^4 M^{-1} (K_D^{app} = 68.1 μM).

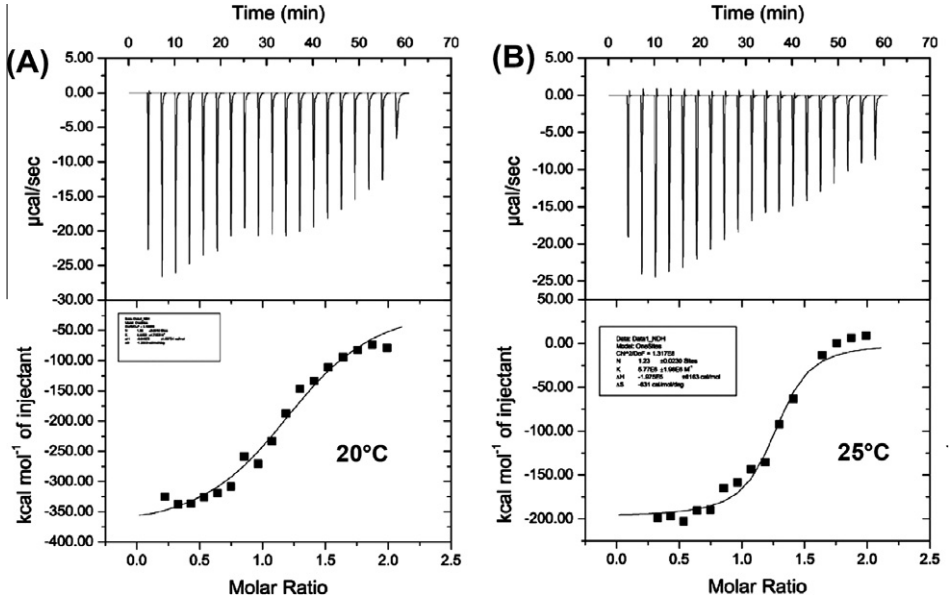

Fig. 2. Calorimetric titration of Grb2-SH2 with ^{P}AICD-47. Reactions were carried out at two different temperatures: (A) 20 °C and (B) 25 °C. Raw data obtained from 20 injections (10 µL each) of ^{P}AICD-47 (120 µM) into 8 µM Grb2-SH2 20 mM Mes, 300 mM NaCl, (pH 6.5) in these two temperatures. Nonlinear least-squares fit of the incremental heat per mole of added ligand for the titration as a function of the molar ratio are also shown here.

Similar high exothermic reaction ($\Delta H = -197.5 \pm 6.2$ kcal mole^{-1}) has been observed at 25 °C (Fig. 2B). The average binding constant at 25 °C (K_B) was $5.77 \pm 1.6 \times 10^6$ M^{-1}, corresponding to a dissociation constant (K_D) of nanomolar order (~173 nM) which is consistent with the earlier reported value of dissociation constant (~220 nM) measured by tryptophan fluorescence quenching method [6]. The corresponding ΔG and ΔS values at 25 °C were −9.2 kcal mol^{-1} and −631 cal mol^{-1}deg^{-1}, respectively. The apparent binding constant (K_B^{app}) was 1.0×10^5 M^{-1} (K_D^{app} = 10.0 µM).

4. Discussion

Intrinsically unstructured proteins show hydrodynamic properties characteristic of random coils or premolten globules with a minimum ordered secondary structure and almost no tightly packed interior [25]. Our current CD data revealed that in the absence of any solvent, at different pH, around ~15–20% fraction of AICD-47 remained as β-strands while the rest of the domain was predominantly random coil. Previously, NMR data of AICD-47 identified two type-1 β-turns, spanning the ^{668}-TPEE-^{671} and ^{684}-NPTY-^{687} motifs which was almost ~16% of full length AICD-47 and rest of the protein was reported to be composed of nascent helix and random coil, with intramolecular long range interaction being almost absent [8]. The transition of the spectral minima of AICD-47 (pI ≈ 7) with pH was expected due to the change of net surface charge of the highly solvent exposed molecule. Helicity of AICD-47 increased almost linearly after addition of TFE. In the present experimental condition, small nascent helices and random coils of AICD-47 present in initial stages, fused together and formed a large single helix in presence of higher amount of TFE concentrations. Apparently, AICD-47 possessed inherent helix forming ability, which was also substantiated in presence of HFIP. Though at initial concentrations, HFIP acted as a better helix inducer as compared to TFE, as number of increasing fluorines directly correlated with its helix inducing efficiency, the transition got saturated at 40% (v/v); beyond which their effects were indistinguishable. However, at low HFIP concentration (20% v/v) some β-sheet content has been found. The β-turns as observed in NMR structure could have been stabilized at this initial stage. Similar HFIP treated β conformations have been observed for Aβ peptides [26]. Interestingly however, change in the relative quantity of α-helicity and β-strands were marginal with changes in solution pH. From its normal cytoplasmic distribution, AICD-47 could relocate into endo-lysosomal pathway having considerably low pH [27]. The fact that structurally AICD-47 remained unchanged in different pH environment indicating that hydrogen ion concentration in a given milieu had relatively less effect on the overall structural module of AICD-47. Overall structural similarity of AICD-47 at three different pH values also indicated a negligible contribution of His-tag in altering the spectroscopic properties of the molecule. Molecular surfaces of binding partners might have pronounced effect on AICD-47 conformations and both TFE and HFIP together provided a noteworthy indication of that possibility.

By ITC experiment at 25 °C, the interaction of ^{P}AICD-47 with Grb2-SH2 domain was found to be exothermic being governed by the enthalpic contribution with almost similar binding constants as obtained before [6]. Tyrosine-phosphorylated AICD derived nona-peptide (-^{679}QNG^{P}YENPTY^{687}-), complexed with Grb2-SH2 domain, revealed an extensive electrostatic interactions between Grb2-SH2 and PTR, Asn and Glu residues of the AICD peptide. The presence of Pro at pY + 3 position in AICD peptide further enhanced the interacting molecular surface. One important feature of Grb2-SH2 domain was its existence both as swapped or non-swapped mediated dimer in solution [28]. In this Grb2-SH2 dimeric surface unstructured ^{P}AICD-47 could undergo a facile transformation into a folded form with the formation of new contacts and unusual high value of enthalpy change probably originated from this structural transition [7]. Number of degrees of freedom of amino acid side chains reduced extensively from its free ^{P}AICD-47 fragment to bound conformation. As a result, the reaction became entropically unfavorable, as reflected in the high negative value of ΔS (−631 cal mol^{-1}deg^{-1}). The large number of hydrogen bonds which were formed during the binding might be a major source of large negative enthalpy change, however, concomitant ordering process associated with the negative entropy change led to enthalpy–entropy compensation. This resulted into a nanomolar dissociation constant ($\Delta G = -9.2$ kcal mol^{-1}). At 20 °C, on the other hand, the free ^{P}AICD-47 was tightly surrounded by more layers of ordered

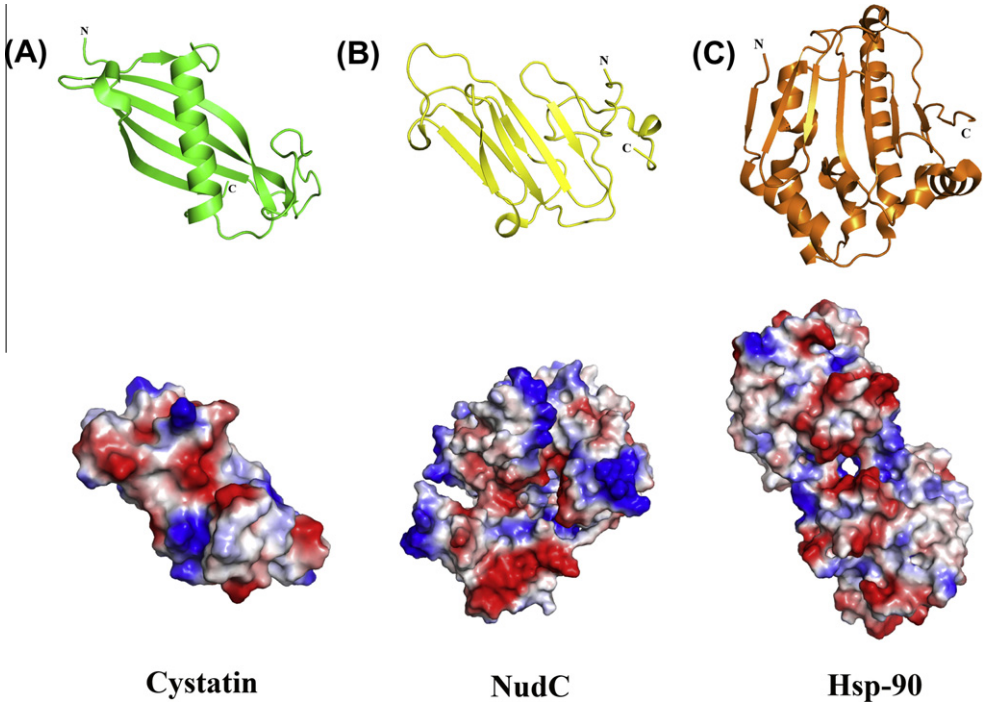

Fig. 3. Diverse structural features of different AICD-47 interactors. (A) cystatins (shown in green ribbon) composed of a central α-helix surrounded by five-stranded antiparallel β sheet (PDB code: 1RN7.pdb). (B) NudC (shown in yellow ribbon), where central part of the molecule contains all-antiparallel β-sandwich, the rest of the molecule is highly flexible (PDB code: 3QOR.pdb). (C) The human Hsp90 N-terminal fragment (shown in orange ribbon) composed of nine helices and an antiparallel β-sheet of eight strands all collectively folds into a α + β sandwich (PDB code: 3HHU.pdb) The molecular surfaces of these interactors are also portrayed here where positive, negative and hydrophobic patches are shown in blue, red and white surface, respectively. (For interpretation of the references to color in this figure legend, the reader is referred to the web version of this article.)

water molecules imposing a shielding effect on the accessibility of Grb2-SH2 domain's binding interface accounting for higher enthalpic contribution through abundant hydrogen bonding with water molecules. The situation was reminiscent of a premolten globule state of the IUD, where the exposed residues were ready to interact but not yet ready to present a complete complimentary binding interface. At 25 °C, the ^{P}AICD-47 was covered with less number of water molecules, could interface with the Grb2-SH2 domain surface competently and better binding had been observed as compared to 20 °C. As cratic water molecules present in the binding interface had definite contribution in overall interaction, we calculated the apparent binding constants (K_B^{app}) of the molecular interaction where contribution of water molecules had been excluded. At both temperatures, significant contribution had been derived from protein–protein as well as water molecule mediated interactions. Molecular recognition mediated by IUDs showed a different paradigm of protein–protein interaction than their more folded counterparts, enthalpy–entropy compensation being a salient thermodynamic feature of the process.

Biophysical parameters, so far observed, indicated a flexible binding interface for AICD-47. Examining the structural features of different categories AICD-47 interactors, the finer intricacies of the IUD interactions can be nicely illustrated. For cystatin D (Fig. 3A), the substrate binding site is composed of three specific fragments: the highly flexible N-terminal region, a hairpin loop present in the central region and another towards the C-terminal end [29]. NudC (Nuclear distribution gene C), on the other hand, lacks secondary structure in a significant portion of the protein while the core of the molecule (158–274) forms an all-antiparallel β-sandwich and a highly conserved yet flexible C-terminal helix (Fig. 3B) [30,31]. Hsp90-β, the classic molecular chaperone with its ATPase activity, is another AICD-47 interactor (Fig. 3C). For *E.coli* Hsp90 homologue the helix H21, an amphiphatic helix positioned towards the dimeric cleft has been anticipated to be a probable binding site for the client unfolded proteins [32]. From all these structural analyses it is obvious that no similar binding surface is present in these distinct AICD-47 binding associates. Naturally, AICD-47 has the potential to fold according to its corresponding binding partner and this is only possible due to its structural flexibility as an IUD.

According to our observations, unstructured AICD-47 works like a "hub" protein like p53, where natively unfolded regions achieve specific conformation after its association with cognate partners and molecular surface of these complexes dictate the conformation [33]. That could precisely be the reason behind altogether different conformers of AICD-47 with Fe65-PTB2 or Grb2-SH2 and their downstream functional consequences. Very interestingly, conformational alterations of AICD-47 are not that pronounced with changes in pH and temperature, indicating that the intrinsic structural dependence is guided solely by binding partners. However, the interaction and conformational switching must be transient enough to engage with next round of interactions with different partners. Intricate balance of these interactions are maintained satisfactorily for IUDs in different cellular processes and it is conjectured that any deviation from this equilibrium generates AD like different neurodegenerative conditions [34].

Acknowledgment

This work was funded by the Structural Proteomics and Genomics of Human Genetic Disorders (SPGHGD) Project, Department of Atomic Energy (DAE), Government of India.

References

[1] B. He, K. Wang, Y. Liu, B. Xue, V.N. Uversky, A.K. Dunker, Predicting intrinsic disorder in proteins: an overview, Cell Res. 19 (2009) 929–949.
[2] V.N. Uversky, Natively unfolded proteins: a point where biology waits for physics, Protein Sci. 11 (2002) 739–756.

[3] P. Tompa, Intrinsically unstructured proteins, Trends Biochem. Sci. 27 (2002) 527–533.
[4] H.J. Dyson, P.E. Wright, Intrinsically unstructured proteins and their functions, Nat. Rev. Mol. Cell Biol. 6 (2005) 197–208.
[5] P. Bowman, C.A. Galea, E. Lacy, R.W. Kriwacki, Thermodynamic characterization of interactions between p27(Kip1) and activated and non-activated Cdk2: intrinsically unstructured proteins as thermodynamic tethers, Biochim. Biophys. Acta 1764 (2006) 182–189.
[6] S. Das, M. Raychaudhuri, U. Sen, D. Mukhopadhyay, Functional implications of the conformational switch in AICD peptide upon binding to Grb2-SH2 domain, J. Mol. Biol. 414 (2011) 217–230.
[7] J. Radzimanowski, B. Simon, M. Sattler, K. Beyreuther, I. Sinning, K. Wild, Structure of the intracellular domain of the amyloid precursor protein in complex with Fe65-PTB2, EMBO Rep. 9 (2008) 1134–1140.
[8] T.A. Ramelot, L.N. Gentile, L.K. Nicholson, Transient structure of the amyloid precursor protein cytoplasmic tail indicates preordering of structure for binding to cytosolic factors, Biochemistry 39 (2000) 2714–2725.
[9] C. McNemar, M.E. Snow, W.T. Windsor, A. Prongay, P. Mui, R. Zhang, J. Durkin, H.V. Le, P.C. Weber, Thermodynamic and structural analysis of phosphotyrosine polypeptide binding to Grb2-SH2, Biochemistry 36 (1997) 10006–10014.
[10] N. Hirota, K. Mizuno, Y. Goto, Cooperative alpha-helix formation of beta-lactoglobulin and melittin induced by hexafluoroisopropanol, Prot. Sci. 6 (1997) 416–421.
[11] F.D. Sonnichsen, J.E. Van Eyk, R.S. Hodges, B.D. Sykes, Effect of trifluoroethanol on protein secondary structure: an NMR and CD study using a synthetic actin peptide, Biochemistry 31 (1992) 8790–8798.
[12] S.R. Lehrman, J.L. Tuls, M. Lund, Peptide alpha-helicity in aqueous trifluoroethanol: correlations with predicted alpha-helicity and the secondary structure of the corresponding regions of bovine growth hormone, Biochemistry 29 (1990) 5590–5596.
[13] P. Kaczka, A. Polkowska-Nowakowska, K. Bolewska, I. Zhukov, J. Poznanski, K.L. Wierzchowski, Backbone dynamics of TFE-induced native-like fold of region 4 of Escherichia coli RNA polymerase sigma70 subunit, Proteins 78 (2010) 754–768.
[14] M. Fandrich, M.A. Fletcher, C.M. Dobson, Amyloid fibrils from muscle myoglobin, Nature 410 (2001) 165–166.
[15] S. Srisailam, T.K. Kumar, D. Rajalingam, K.M. Kathir, H.S. Sheu, F.J. Jan, P.C. Chao, C. Yu, Amyloid-like fibril formation in an all beta-barrel protein. Partially structured intermediate state(s) is a precursor for fibril formation, J. Biol. Chem. 278 (2003) 17701–17709.
[16] W.C. Wigley, S. Vijayakumar, J.D. Jones, C. Slaughter, P.J. Thomas, Transmembrane domain of cystic fibrosis transmembrane conductance regulator: design, characterization, and secondary structure of synthetic peptides m1–m6, Biochemistry 37 (1998) 844–853.
[17] S. Segawa, T. Fukuno, K. Fujiwara, Y. Noda, Local structures in unfolded lysozyme and correlation with secondary structures in the native conformation: helix-forming or -breaking propensity of peptide segments, Biopolymers 31 (1991) 497–509.
[18] L.V. Najbar, D.J. Craik, J.D. Wade, D. Salvatore, M.J. McLeish, Conformational analysis of LYS(11–36), a peptide derived from the beta-sheet region of T4 lysozyme, in TFE and SDS, Biochemistry 36 (1997) 11525–11533.
[19] K. Yanagi, M. Ashizaki, H. Yagi, K. Sakurai, Y.H. Lee, Y. Goto, Hexafluoroisopropanol induces amyloid fibrils of islet amyloid polypeptide by enhancing both hydrophobic and electrostatic interactions, J. Biol. Chem. 286 (2011) 23959–23966.
[20] S.K. Pachahara, N. Chaudhary, C. Subbalakshmi, R. Nagaraj, Hexafluoroisopropanol induces self-assembly of beta-amyloid peptides into highly ordered nanostructures, J. Pept. Sci. 18 (2012) 233–241.
[21] R. Bhandari, R. Mathew, K. Vijayachandra, S. Visweswariah, Tyrosine phosphorylation of the human guanylyl cyclase C receptor, J. Biosci. 25 (2000) 339–346.
[22] C. Louis-Jeune, M.A. Andrade-Navarro, C. Perez-Iratxeta, Prediction of protein secondary structure from circular dichroism using theoretically derived spectra, Proteins 80 (2012) 374–381.
[23] A.L. Lai, H. Park, J.M. White, L.K. Tamm, Fusion peptide of influenza hemagglutinin requires a fixed angle boomerang structure for activity, J. Biol. Chem. 281 (2006) 5760–5770.
[24] J.P. Waltho, V.A. Feher, G. Merutka, H.J. Dyson, P.E. Wright, Peptide models of protein folding initiation sites. 1. Secondary structure formation by peptides corresponding to the G- and H-helices of myoglobin, Biochemistry 32 (1993) 6337–6347.
[25] V.N. Uversky, What does it mean to be natively unfolded?, Eur J. Biochem. 269 (2002) 2–12.
[26] S. Tomaselli, V. Esposito, P. Vangone, N.A. van Nuland, A.M. Bonvin, R. Guerrini, T. Tancredi, P.A. Temussi, D. Picone, The alpha-to-beta conformational transition of Alzheimer's Abeta-(1–42) peptide in aqueous media is reversible: a step by step conformational analysis suggests the location of beta conformation seeding, Chembiochem 7 (2006) 257–267.
[27] M. Raychaudhuri, D. Mukhopadhyay, Grb2-mediated alteration in the trafficking of AbetaPP: insights from Grb2-AICD interaction, J. Alzheimers Dis. 20 (2010) 275–292.
[28] N. Schiering, E. Casale, P. Caccia, P. Giordano, C. Battistini, Dimer formation through domain swapping in the crystal structure of the Grb2-SH2-Ac-pYVNV complex, Biochemistry 39 (2000) 13376–13382.
[29] M. Alvarez-Fernandez, Y.H. Liang, M. Abrahamson, X.D. Su, Crystal structure of human cystatin D, a cysteine peptidase inhibitor with restricted inhibition profile, J. Biol. Chem. 280 (2005) 18221–18228.
[30] M. Zheng, T. Cierpicki, A.J. Burdette, D. Utepbergenov, P.L. Janczyk, U. Derewenda, P.T. Stukenberg, K.A. Caldwell, Z.S. Derewenda, Structural features and chaperone activity of the NudC protein family, J. Mol. Biol. 409 (2011) 722–741.
[31] X.J. Zhu, X. Liu, Q. Jin, Y. Cai, Y. Yang, T. Zhou, The L279P mutation of nuclear distribution gene C (NudC) influences its chaperone activity and lissencephaly protein 1 (LIS1) stability, J. Biol. Chem. 285 (2010) 29903–29910.
[32] A.K. Shiau, S.F. Harris, D.R. Southworth, D.A. Agard, Structural analysis of *E. coli* hsp90 reveals dramatic nucleotide-dependent conformational rearrangements, Cell 127 (2006) 329–340.
[33] B. Vogelstein, D. Lane, A.J. Levine, Surfing the p53 network, Nature 408 (2000) 307–310.
[34] S. Das, D. Mukhopadhyay, Intrinsically unstructured proteins and neurodegenerative diseases: conformational promiscuity at its best. IUBMB Life 63 (2011) 478–488.